THE ASTROPHYSICAL JOURNAL, 474:741–748, 1997 January 10

BIG GRAINS IN THE RED RECTANGLE?

M. JURA, J. TURNER, AND S. P. BALM
Department of Physics and Astronomy, University of California, Los Angeles CA 90095-1562;
jura@clotho.astro.ucla.edu, chicag@jean.astro.ucla.edu, balm@gentoo.spole.gov
Received 1996 January 22; accepted 1996 July 25

ABSTRACT

We report VLA observations at 3.6 cm, 2 cm, and 1.3 cm of the Red Rectangle and Hα spectroscopy of HD 44179, the central binary star in the nebulosity. Emission is detected at all three radio wavelengths, and the source is resolved at 2 cm and 1.3 cm. Convolved to the same beam, the radio spectrum of the inner 0″.76 × 0″.49 is characteristic of thermal emission from ionized gas which becomes optically thin near 2 cm. The diameter of the bulk of the ionized gas producing this radio emission is between 1.3×10^{14} cm (∼10 AU) and 2×10^{15} cm (∼100 AU); in this region we estimate that 10^6 cm$^{-3} \leq n_e \leq 4 \times 10^6$ cm^{-3}. The Hα profile has both a wide (200 km s^{-1} full-width zero-intensity) plateau which is probably associated with a small circumstellar region ($<10^{13}$ cm or ∼1 AU) and a spike (FWHM ≈ 20 km s^{-1}) which we suggest is produced in the extended ionized gas ($\geq 10^{14}$ cm) detected at radio wavelengths.

We also detect low surface brightness radio emission at 2 cm and 1.3 cm, but not at 3.6 cm, that is extended well beyond 1″ from the source. This extended radio emission has a spectral index between 1.3 cm and 3.6 cm greater than 3.2 and is therefore produced by grains. Our VLA data also indicate that the previously observed millimeter continuum flux cannot result from ionized gas and therefore is emitted by dust. Although uncertain, it is possible that the centimeter and millimeter wavelength continuum arise from the same dust, in which case there is probably little frequency variation in the emissivity of the dust between 1.3 cm and 0.13 cm. We propose that there is an orbiting, long-lived gravitationallly bound disk of dust grains with radii ≥0.02 cm.

Subject headings: dust, extinction — ISM: clouds — ISM: individual (Red Rectangle) — radio continuum: ISM — stars: AGB and post-AGB

1. INTRODUCTION

In order to understand better the formation of planets, we are studying environments where small particles can coagulate and grow. One such location is a dust-containing circumstellar disk where the grain-grain collision time is shorter than the disk lifetime. Most previous studies of such disks have focused on those around pre–main-sequence stars, but some post–main-sequence stars also possess dusty disks (Waters et al. 1993). The best current model for the Red Rectangle is that it contains a carbon-rich post–asymptotic giant branch (AGB) star which is evolving into the planetary nebula phase (van Winckel, Waelkens, & Waters 1995; Roddier et al. 1995), and there is good evidence for a long-lived disk around this star.

Mass-losing red giants such as IRC +10216 form dust in their cool, dense winds. However, under the assumption that the particles are spherical, most of the mass in these grains is found in objects with radii less than 0.1 μm (Martin & Rogers 1987; Griffin 1990; Jura 1994; Ivezic & Elitzur 1996). In contrast, there may be at least a few evolved stars with larger grains in their circumstellar environments (Skinner 1994; Shenton, Evans, & Williams 1995, Lissauer et al. 1996), and it has been suggested that there might be many grains with radii larger than 0.02 cm in the Red Rectangle (Jura, Balm, & Kahane 1995). Here, we explore further this hypothesis.

The Red Rectangle reflection nebulosity was first studied by Cohen et al. (1975) who recognized from the RAFGL survey (see Price 1988) that the central star, HD 44179, is a powerful infrared source. The Red Rectangle displays axial symmetry on the sky and emits strong infrared bands (Léger & Puget 1983; Bregman et al. 1993), a set of unidentified optical bands at wavelengths longward of 5800 Å (Schmidt, Cohen, & Margon 1980), and CH^+ (Balm & Jura 1992). The reflected light displays an X-shaped morphology on scales of both 10″ (Schmidt & Witt 1991) and 0″.1 (Roddier et al. 1995) although with a wider opening angle on the large scale. The Red Rectangle is sufficiently puzzling that there have been recent proposals for either a hitherto undetected red star (Roddier et al. 1995) or an as yet undetected blue star (Knapp et al. 1995).

Van Winckel et al. (1995) have found that HD 44179 is a spectroscopic binary with a 298 day period. Jura et al. (1995) have detected circumstellar CO emission with a velocity width considerably narrower than the velocity range displayed by HD 44179 in its binary motion, and they argued that the most plausible interpretation of the CO velocity profile is that it signals the presence of a long-lived orbiting disk. In order to remain gravitationally bound, many of the dust particles in this disk may have radii in excess of 0.02 cm.

In the atmosphere of the A-type star HD 44179, carbon, nitrogen, and oxygen are near solar in abundance, but there is a deficiency by about a factor of 1000 in the abundances of refractory elements such as iron that are normally contained within dust particles (Waelkens et al. 1992; Van Winckel, Mathis, & Waelkens 1992). Accretion of gas but not dust from a long-lived disk can explain why the abundances in the atmosphere of HD 44179 are so peculiar (Mathis & Lamers 1992; Waters, Trams, & Waelkens 1992).

An unsolved mystery regarding the Red Rectangle is that it emits at 1 mm nearly 10 times more energy than expected on the basis of simple models for the circumstellar dust (Walmsley et al. 1991; van der Veen et al. 1994). It is possible that this millimeter continuum is produced by large circumstellar dust particles as occurs for pre–main-sequence stars (see, for example, Mannings & Emerson 1994; Koerner, Chandler, & Sargent 1995), but this is uncertain. Shenton et al. (1995) have proposed that there are large grains near 89 Her and AC Her to explain the millimeter continua from these stars. However, at least in the case of 89 Her, there is an outer extended shell of gas (Alcolea & Bujarrabal 1995) which could contain a significant number of cold grains that might mimic the emission from a population of large grains. Although other post–main-sequence stars exhibit a millimeter continuum in excess of that predicted for simple models (van der Veen et al. 1995), at least in some cases this might be from underestimating the emission from the extended photosphere which can be stronger than predicted at centimeter wavelengths (Reid & Menten 1995).

In order to develop a better understanding of the Red Rectangle, we have obtained both VLA[1] images of the system and a high-resolution optical spectrum of HD 44179. Knapp et al. (1994) have reported extended grain emission at 3.6 cm from RAFGL 2688 (the Egg Nebula), another carbon-rich pre–planetary nebula, and we have searched for such emission from the Red Rectangle. The data and analysis are reported below.

2. OBSERVATIONS AND RESULTS

2.1. *Radio Data*

We obtained the VLA data on 1995 September 26 using a BnA configuration and observing for about an hour each at 3.6 cm, 2 cm, and 1.3 cm in acceptable quality weather. At each wavelength, we used two receivers of slightly different central frequencies with bandwidths of 50 MHz and with both right and left circular polarizations. Fluxes were bootstrapped in the usual manner from 3C 147 with adopted fluxes of 4.58, 2.51, and 1.59 Jy at 3.6, 2, and 1.3 cm, respectively. We interleaved observations of the Red Rectangle with the nearby quasar 0607−085 every 20 minutes. The data were reduced at UCLA using the standard AIPS package. After calibration, maps were made with natural weighting, and for the 1.3 cm map, a slight taper (900 kλ) was applied to improve the signal-to-noise. Due to lack of short baselines, the maps are not sensitive to extended emission: undersampling affects the maps at size scales of 20″, 12″, and 7″ at 3.6 cm, 2 cm, and 1.3 cm, respectively.

The 3.6 cm map is shown in Figure 1. The source may be slightly resolved with an elliptical shape of 0″.33 × 0″.12 at a position angle of 160°–170° as deconvolved from the elliptical beam of 0″.76 × 0″.49 at position angle −87°. The peak flux density is 0.43 mJy beam^{-1}, with an rms uncertainty of 0.022 mJy beam^{-1}. We also list in Table 1 the fluxes derived in larger circular beams with values of the FWHM ranging from 1″ to 3″.5. Our measured flux agrees with the previous measurements of 0.44 mJy by Knapp et al. (1995) or 0.48 mJy by Claussen & Beasley (1995). Because these previous measurements were obtained with the VLA in a more compact configuration, it seems that there is little extended emission from the Red Rectangle at 3.6 cm, consistent with our analysis.

[1] The VLA of the National Radio Astronomy Observatory is operated by Associated Universities Inc. under cooperative agreement with the National Science Foundation.

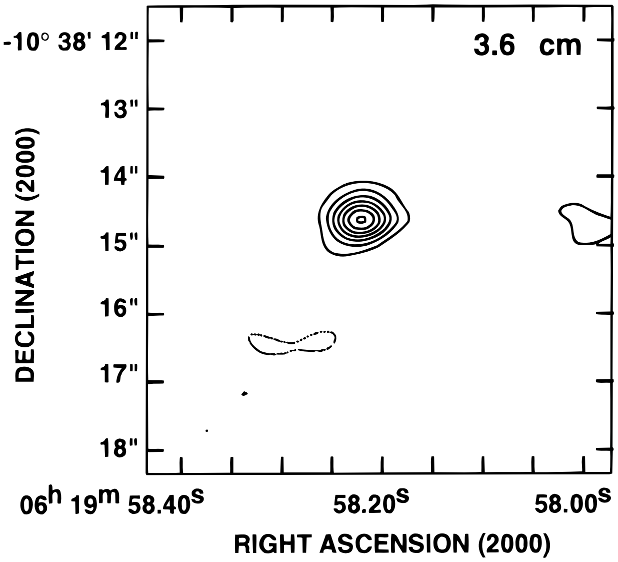

FIG. 1.—Map of the 3.6 cm emission from the Red Rectangle; the elliptical beam is 0″.76 × 0″.49, p.a. −87°. The contours are plotted at 2 σ levels where 2 σ = 6.0 × 10^{-5} Jy beam^{-1}.

Our measured radio position is α(2000.0) = 6^{h}19^{m}58^s.220 ± 0^s.001; δ(2000.0) = −10°38′14″.57 ± 0″.01. Corrected for proper motion to 1995.7, the optical position of HD 44179 given in the Position and Proper Motion Catalog is α(2000.0) = 6^{h}19^{m}58^s.206 ± 0^s.004; δ(2000.0) = −10°38′14″.69 ± 0″.06. Because the optical light is scattered off nebulosity which is separated by ∼0″.1 from the star (Roddier et al. 1995), the disagreement of 0″.24 between the optical and radio positions may be real.

Unlike the 3.6 cm emission, the 2 cm emission is clearly extended as can be seen in Figure 2. The beam for this map is 0″.42 × 0″.37, position angle 78°, and the rms noise level is 0.07 mJy beam^{-1}. There is a core source of flux density 0.69 mJy beam^{-1}, coincident within 0″.02 with the 3.6 cm peak, and there is an extension to the northeast of the main peak. The total fluxes in different beams are listed in Table 1.

The 1.3 cm map is shown in Figure 3. The map has a synthesized beam of 0″.40 × 0″.29 at position angle 7°; the rms noise level is 0.12 mJy beam^{-1}. The peak flux density is 0.83 mJy beam^{-1}, spatially coincident with the peaks in the 3.6 and 2 cm maps. As can be seen in Figure 3 there is a clear extension to the north of the main continuum source with a flux in the secondary peak of 0.55 mJy or the 4.5 σ level. In addition, based on the large number of extended

TABLE 1

RADIO FLUXES FROM THE RED RECTANGLE

BEAM (FWHM) (arcsec)	FLUX (mJy)		
	3.6 cm	2.0 cm	1.3 cm
0.76 × 0.49	0.43	0.69	0.83
1	0.49	1.09	1.07
2	0.52	1.3	1.71
3	0.49	1.44	2.37
3.5	0.47	1.5	2.6
Maximum	0.58	2.1	3.9

NOTE.—The fluxes are measured for the central region at maps convolved to the given beam size, except for the last row which is simply the maximum flux in the entire VLA map at each frequency.

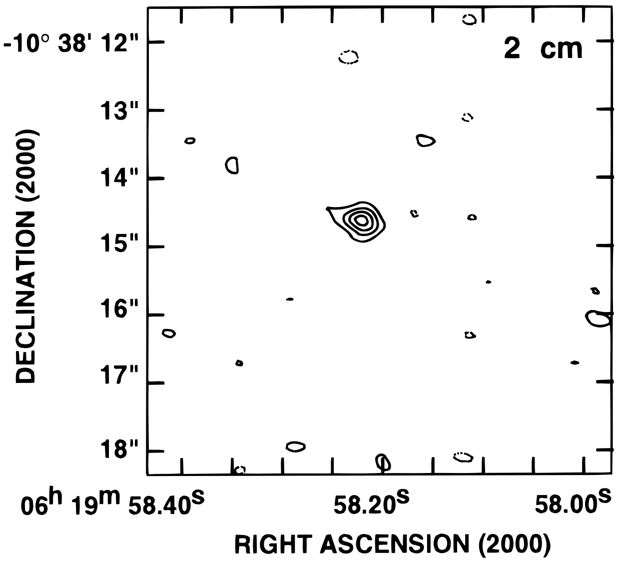

FIG. 2.—Map of the 2 cm emission from the Red Rectangle; the elliptical beam is 0."42 × 0."37, p.a. 78°. The contours are plotted at 2 σ levels where 2 $\sigma = 2.0 \times 10^{-4}$ Jy beam^{-1}.

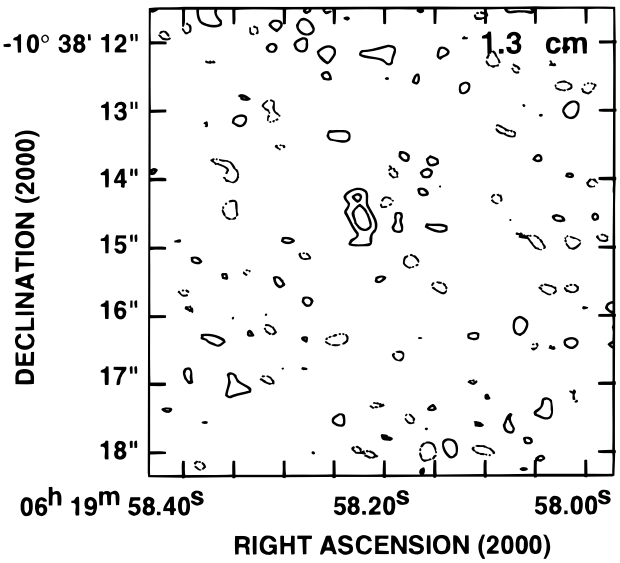

FIG. 3.—Map of the 1.3 cm emission from the Red Rectangle; the elliptical beam is 0."40 × 0."29, p.a. 7°. The contours are plotted at 2 σ levels where 2 $\sigma = 2.5 \times 10^{-4}$ Jy beam^{-1}. The preponderance of positive contours beyond the compact source probably indicates the presence of undersampled extended emission, particularly in an east–west ridge ~3" north of the main continuum source.

2 σ positive contours, there appears to be extended emission at 1.3 cm that is undersampled in the present map. Fluxes in different synthesized beams listed in Table 1 indicate that the emission is clearly extended.

As shown in Figure 4*a* where the data for the two frequencies are compared, at 1.3 cm, there is the hint of an extension to the west of the source which is not seen at 2 cm. If real, this extension might be emission from dust in the disk.

In the compact core source, the spectral index of the radio emission between 3.6 cm and 1.3 cm is 1.5; the emission is probably produced by ionized gas which becomes optically thin near 2 cm. In an annulus with inner diameter of 1" and outer diameter of 3."5, the flux at 1.3 cm is 1.8 mJy, while the upper limit to the flux at 3.6 cm is 0.07 mJy so that the spectral index of the emission is $\geq$3.2. This extended emission is almost certainly produced by dust. As shown in Figure 4*b*, although the positional registration is uncertain, the agreement between the morphology of the 1.3 cm map and that of the 1.65 μm emission, which is produced by scattering from dust grains, also suggests that the extended emission at 1.3 cm is produced by dust.

2.2. *Optical Data*

Optical spectra of HD 44179 were obtained on 1994 January 3 using the Hamilton echelle spectrograph on the 3 m telescope at Lick Observatory. The slit width of 800 μm allowed us to obtain a spectral resolution of 6 km s^{-1} as

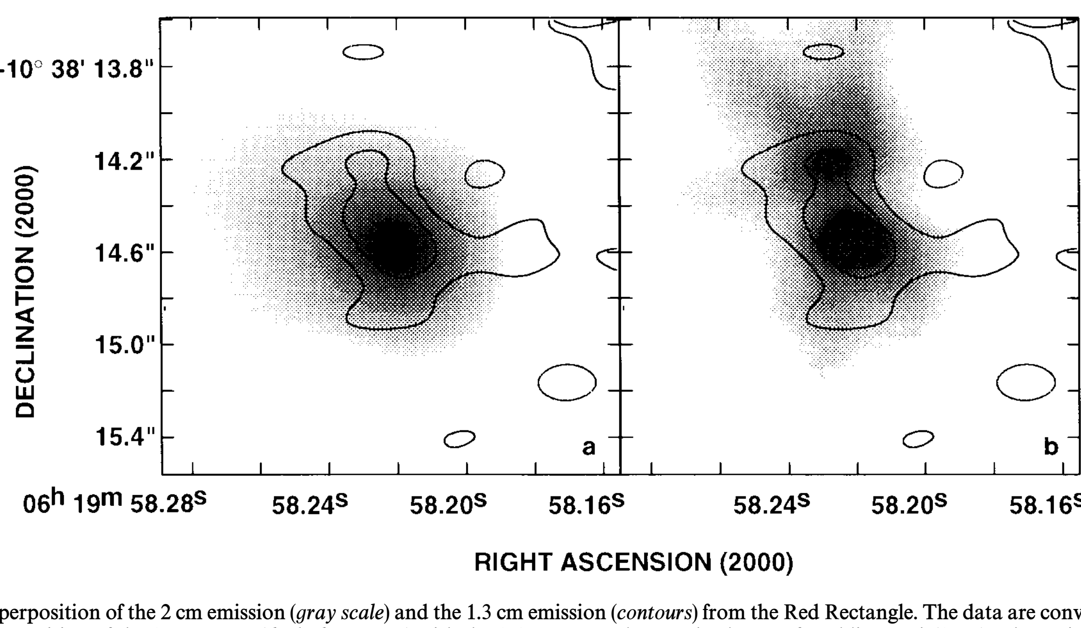

FIG. 4.—(*a*) Superposition of the 2 cm emission (*gray scale*) and the 1.3 cm emission (*contours*) from the Red Rectangle. The data are convolved to the same beam size. (*b*) Superposition of the 1.3 cm map (*dashed contours*) with the 1.65 μm map deconvolved map of Roddier et al. (1995). The registration of the two images is not certain because we do not know the absolute pointing for the infrared data, but there does appear to be good agreement between the morphology of the two maps as presented.

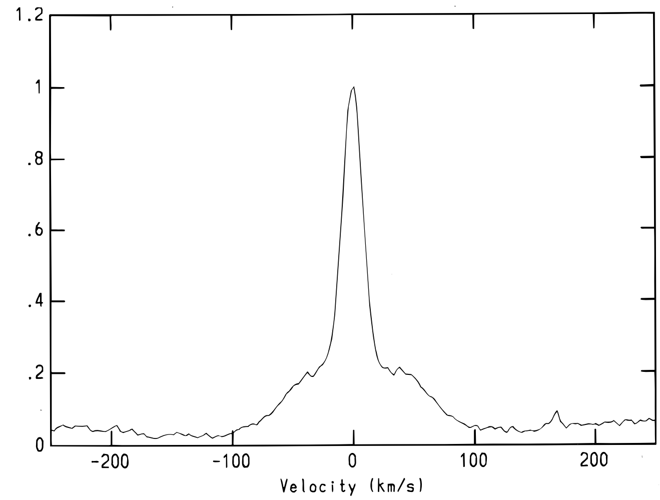

FIG. 5.—The Hα emission line for HD 44179; the continuum level is defined at intensity 0.0 to present a full display of the line profile.

measured from the calibration lines of the thorium argon lamp. The data were reduced at UCLA using IRAF.

In Figure 5, we display the Hα line profile for HD 44179. The line is symmetric and consists of a spike sitting on top of a broad plateau. The equivalent width of the entire feature is 3.5 Å. The narrow spike has a measured LSR velocity of 3.4 km s^{-1} (21.7 km s^{-1} heliocentric) and a resolved FWHM of 20 km s^{-1}. Within the uncertainties, the plateau has the same radial velocity as does the spike, while emission in the plateau can be traced to ± 100 km s^{-1}. The LSR velocity in the Hα spike is slightly larger than the value of 0.5 km s^{-1} found for the circumstellar CO emission (Jura et al. 1995) but agrees within 0.2 km s^{-1} of the radial velocity found for other narrow emission lines (Van Winckel et al. 1995), which do not follow the orbital motion of HD 44179. As described below, our measurement of a total equivalent width of Hα of 3.5 Å corresponds to a line flux at the Earth of 1.2 photons cm^{-2} s^{-1}.

In reviewing the observations obtained on 1979 December 26 which were reported by Schmidt et al. (1980), G. D. Schmidt (1995) remeasured the flux of Hα and found a value of 0.55 photons cm^{-2} s^{-1}, about a factor of 2 lower than we measured. The spectral resolutions of the two different measurements are not the same, and we do not know whether the apparent difference in the Hα flux is the result of variation in the broad plateau, the spike, or simply observational error. It is possible that during the past 15 yr there has been a factor of 2 increase in the amount of ionization.

3. MODEL OF THE CIRCUMSTELLAR IONIZED GAS

The distance of the Red Rectangle is quite uncertain. Cohen et al. (1975) suggested 330 pc which we adopt here; this distance implies a luminosity of 1000 $L_\odot$. It is entirely possible that the star is as distant as 1000 pc with a luminosity of 10^4 $L_\odot$ (e.g., Knapp et al. 1995). In view of the low gravity (perhaps $\log g = 1.4$ cgs, where $g = GM_*/R_*^2$ although this is difficult to determine, Greenstein & Oke 1977), effective temperature ($T_* = 8000$ K) and mass (~ 1 $M_\odot$) derived for HD 44179 (Waelkens et al. 1992; Van Winckel et al. 1995), the nominal luminosity ($L = 4\pi R_*^2 \sigma_{SB} T_*^4$) is 4000 $L_\odot$. Therefore, it is unlikely that the star lies any nearer than 330 pc. One argument against the larger distance is that in the PPM catalog, the proper motion of HD 44179 is given as 0.029″ yr^{-1} which translates into transverse speeds of 45 km s^{-1} and 137 km s^{-1} at 330 pc and 1000 pc, respectively. In view of the relatively small radial velocity of this star, the smaller transverse velocity seems to be more likely.

In Figure 6, we show the broadband energy distribution of the Red Rectangle for its radio and infrared emission. The integrated radio fluxes from the compact core display a spectrum similar to that of an H II region which becomes optically thin at wavelengths short of 2 cm. In contrast, the extended radio emission is probably produced by dust.

If we consider only the emission from the inner compact core and if $T = 7500$ K, then using the free-free emissivity for an ionized gas of pure hydrogen given by equation (3-54) of Spitzer (1978), the observed flux at 1.3 cm of 0.83 mJy implies that $n_e^2 V = 3.4 \times 10^{55}$ cm^{-3}. Assuming a recombination rate for hydrogen of 3.3×10^{-13} cm^3 s^{-1} (Hummer & Storey 1987) and an average of 20 eV per ionization, then the inferred ionization rate is 1.1×10^{43} s^{-1} while the inferred luminosity in the Lyman continuum is 0.09 $L_\odot$.

The cause of the ionized hydrogen is unknown. The spike profile is so narrow that shock excitation does not seem likely. As can be seen from the ultraviolet spectra at

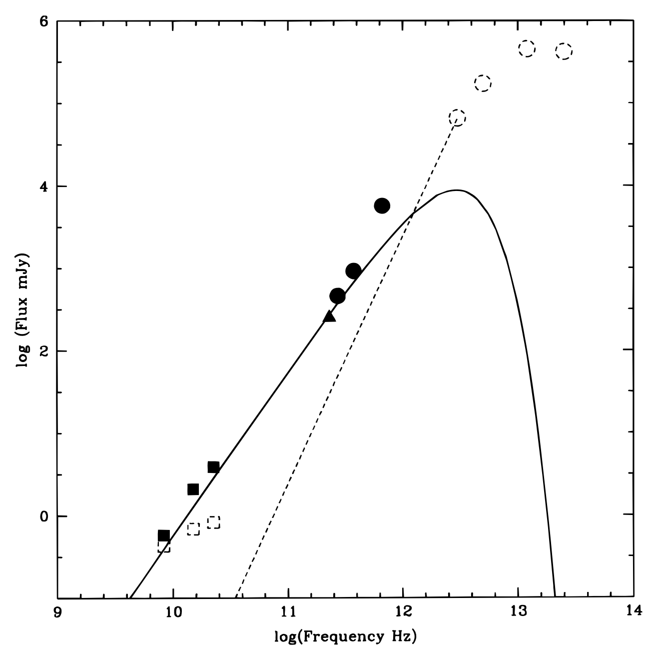

FIG. 6.—A plot of F_ν vs. ν. The radio data (*squares*) are taken from Table 1 of this paper; the error bars are smaller than the symbols. The filled boxes denote the extended radio fluxes (totals given in the bottom line of Table 1) while the open boxes denote the compact radio fluxes from Table 1. The extended radio fluxes do not include emission at angular scales larger than 7″ and are therefore lower limits. The millimeter and submillimeter fluxes are taken from Walmsley et al. (1991) (*triangle*) and Van der Veen et al. (1994) (*filled circles*) while points for the infrared fluxes are from *IRAS* (*open circles*). The solid line is a Planck function for $T = 50$ K scaled so that $F_\nu(1.3\ \text{cm}) = 3$ mJy. The dashed line shows a simple power-law extrapolation of F_ν varying as ν^{+3} from the value of the flux measured by *IRAS* at 100 μm. As discussed in the text, the points for the compact radio source are explained by ionized gas while the infrared points at $\lambda < 100$ μm are explained by the same grains that produced the observed reflection nebula. We suggest that the millimeter and extended centimeter wavelength radio fluxes might result from emission by a distinct population of cold, large particles.

$\lambda > 1200$ Å measured by Sitko, Savage, & Measde (1981) and Sitko (1983), there is no reason to think that HD 44179 emits much Lyman-continuum radiation from its photosphere. Knapp et al. (1995) note that there is more radio continuum emission than would be expected from an A-type star similar to HD 44179, so they suggest that there may be another blue-type star within the system. Alternatively, since HD 44179 displays Hα and He I 10830 Å in emission (Kelly & Latter 1995), we suggest that the Red Rectangle may contain a source of ionization similar to that found in Herbig Ae stars (e.g., Hillenbrand et al. 1992). While we think that the Red Rectangle is a post–main-sequence star, we note that its radio luminosity at 3.6 cm of 6×10^{16} ergs s^{-1} Hz^{-1} is close to the value expected for a pre–main-sequence star whose bolometric luminosity is 10^3 $L_\odot$ (Fig. 19, Skinner, Brown, & Stewart 1993). One possibility is that accretion onto either HD 44179 or its companion at a rate near 10^{-8} $M_\odot$ yr^{-1} could result in Lyman-continuum emission as such accretion rates produce substantial Lyman α emission (Blondel, Talavera, & Djie 1993). Whatever the process that produces the ionization in pre–main-sequence environments may be operating around the Red Rectangle as well, and there may not be an additional hot star in the system.

If the ionized gas has an (uncertain) kinetic temperature of 7,500 K, the observed flux at 3.6 cm which appears to be produced by an optically thick region requires that the ionized gas subtend a solid angle of 2.7×10^{-14} sr. This solid angle implies that the minimum diameter of the gas is 2×10^{14} cm ($\sim$10 AU). (This size is comparable to that found for the ionized gas around Be stars [Taylor et al. 1990].)

The plateau and the spike in the Hα line are probably produced in physically distinct regions. The speed of the gas in the plateau is as high as ± 100 km s^{-1} which is much larger than the amplitude of 26 km s^{-1} displayed by HD 44179 in its binary motion. Therefore, the gas producing the broad plateau is probably largely confined to a diameter smaller than 10^{13} cm ($\sim$1 AU) which implies a solid angle as seen from Earth of less than 10^{-16} sr. Such a confined volume of ionized gas at 7500 K could produce a flux at Earth at 3.6 cm of only 0.002 mJy, a factor of $\sim$200 smaller than the observed flux. In contrast, we now argue that the more slowly moving gas detected in the spike of the Hα profile is almost certainly substantially farther from the star than 10^{14} cm ($\sim$10 AU). While we do not know the physical cause of the broadening of the spike profile, we can assume that the upper limit to the orbital velocity, V_{orb}, is 10 km s^{-1} since the observed FWHM of the line is 20 km s^{-1}. Because the total mass of the central binary, M_{tot}, is between 1.0 and 1.5 $M_\odot$ (Van Winckel et al. 1995), the ionized gas may be located at a distance $\geq (GM_{tot})/V_{orb}^2$ or more than 1.3×10^{14} cm, corresponding to an angular radius of 0\".04, consistent with the minimum radio size derived above. Van Winckel et al. (1995) report that the narrow emission lines do not change radial velocity during the orbital period of HD 44179 as expected if they are emitted outside of the binary system.

We can use the optical data also to constrain the rate of hydrogen ionization. The equivalent width of the narrow spike in the Hα emission is about 1.7 Å or about half of the total equivalent width in the entire emission line. Because Cohen et al. (1975) measured $m_V = 8.83$ mag while Van Winckel (1995) reports more recent data with m_V ranging from between 8.80 mag and 8.95 mag, it seems that the continuum flux from the star has not changed much during the past 20 yr. Therefore, we use the Johnson *R*-band magnitude of 8.27 mag measured by Cohen et al. (1975) to estimate the flux in Hα from its equivalent width, together with the calibration that 0.00 mag at *R* band corresponds to 3010 Jy (Johnson 1966). Our measured Hα equivalent width in the spike corresponds to a flux of 0.58 photons cm^{-2} s^{-1}. If the rate of recombination that produces an Hα photon is 1.1×10^{-13} cm^3 s^{-1} (Hummer & Storey 1987) then, in the absence of reddening, we infer that $n_e^2 V = 6.3 \times 10^{55}$ cm^{-3}, about a factor of 2 larger than the value derived from the radio measurements of the compact source.

From our radio measurement that the bulk of the emission from the compact ionized gas has an angular diameter less than 0\".5, then the spatial extent, *L*, of the ionized gas is $\leq 2 \times 10^{15}$ cm ($\sim$100 AU). Above, we showed that the data for the optically thick emission implies that $L \geq 1.3 \times 10^{14}$ cm ($\sim$10 AU). Because the gas becomes optically thin near 2 cm, we find from equation (3-57) in Spitzer (1978) that $n_e^2 L \sim 2 \times 10^{27}$ cm^{-5} (or 6×10^8 cm^{-6} pc). Therefore, we find that 10^6 $cm^{-3} \leq n_e \leq 4 \times 10^6$ cm^{-3}. At this density, forbidden optical emission lines are detectable and in fact have been observed (e.g., Van Winckel et al. 1995).

Our estimate that the ionized gas lies $\sim 10^{15}$ cm from the central binary is the same distance that Balm & Jura (1992) inferred was the separation between the zone where the CH^+ is found and HD 44179. This coincidence naturally occurs in a photodissociation region lying just outside an H II region. Tielens & Hollenbach (1985) have constructed models for photodissociation fronts, and for a gas with $n = 2.3 \times 10^5$ cm^{-3} and an ultraviolet flux of 160 ergs cm^{-2} s^{-1}, the predicted column density for CH^+ is 1.8×10^{12} cm^{-2}. Balm & Jura (1992) argued that the CH^+ in the Red Rectangle is formed in an environment where at 10 eV, the ultraviolet flux is 8000 ergs cm^{-2} s^{-1}, while, as suggested above, the density in the ionized gas near the front is $\geq 10^6$ cm^{-3}. Given that these inferred physical conditions in the CH^+ containing zone are about a factor of 10 different from those used in the model computed by Tielens & Hollenbach (1985), it may be possible that the column density of CH^+ produced in the front is near 10^{13} cm^{-2}, as required to account for the observed fluorescent emission.

If the ionized gas is located at $\sim 10^{15}$ cm ($\sim$60 AU) from the star and if it is moving less than 10 km s^{-1}, the upper limit to the bulk speed we infer from the FWHM of the line, then the timescale for expansion is $\geq$40 yr. Because the Hα flux may have doubled during the past 15 yr, it is possible that the Red Rectangle is in a phase where it is undergoing rapid post-AGB evolution as is apparently the case for RAFGL 618 (Knapp et al. 1995). Although the optical brightness has not changed notably during the past 20 yr, there are similar time intervals when rapidly evolving post-AGB stars do not appreciably change their optical magnitudes (Gottlieb & Liller 1976).

4. MODEL FOR THE DUST

4.1. *Constraints*

One possible explanation for the strong millimeter continuum from the Red Rectangle is that this flux is produced by ionized gas. However, as displayed in Figure 6, it seems that the radio spectrum of the compact emission turns over near 2 cm and the millimeter continuum is not produced by this ionized gas. Furthermore, if the millimeter continuum were produced by ionized gas, the Hα line would be 1000 times stronger than calculated above and would produce an optical emission line much stronger than observed. Because the spectral index of the extended centimeter wavelength flux is ≥ 3.2, this emission is produced by dust, and it is possible but unproven that this same dust produces the millimeter continuum.

Even with complex geometries and time-varying mass loss, standard models for the dust emission from circumstellar envelopes do not reproduce the millimeter and submillimeter fluxes observed for the Red Rectangle (Alcolea & Bujarrabal 1991; Walmsley et al. 1991; Van der Veen et al. 1994; Lopez, Mékarnia, & Lefèvre 1995). The basic difficulty is that within the 24″ beam of the 1.3 mm observations at the SEST (Walmsley et al. 1991) or the 18″ beam of the 1.1 mm measurements at the JCMT (Van der Veen et al. 1994), the small grains used in these models are predicted to be both too hot and to emit too efficiently at 100 μm, relative to their emissivity at 1300 μm, to be able to reproduce the observed ratio $F_\nu(100\ \mu\mathrm{m})/F_\nu(1300\ \mu\mathrm{m}) = 250$. (Because the aperture on *IRAS* used to detect the 100 μm emission was much larger than the beam used with the ground-based telescopes to measure the 1300 μm flux, the discrepancy between the observed and predicted flux ratios cannot be explained as a result of observing more cold grains at a large distance from the star that emit only at 1300 μm.) For example, in the model of Van der Veen et al. (1994) if $\phi('')$ is the angular displacement from HD 44179 as seen from the Earth, then the dust particles illuminated by the observed radiation field in the system have a temperature, T_{gr} in the outer envelope given by:

$$T_{\mathrm{gr}} = 150\ \phi^{-0.38} . \quad (1)$$

From an optically thin cloud, we expect that

$$F_\nu \sim Q_\nu B_\nu(T_{\mathrm{gr}}) . \quad (2)$$

Since Q_ν varies at least as rapidly as ν^{+1} for standard grains, then if the gas temperature is 100 K, the predicted value of $F_\nu(100\ \mu\mathrm{m})/F_\nu(1300\ \mu\mathrm{m}) = 1200$ in marked contrast to the observed value of 250.

As can be visualized from Figure 6, we find that the emission at millimeter and submillimeter wavelengths cannot be explained by an extrapolation either from longer or from shorter wavelengths; therefore we look for another explanation for this emission. Although it is imaginable that the millimeter and submillimeter flux is the blend of many different spectral lines, this possibility seems unlikely in view of the very narrow width of the CO emission (Jura et al. 1995).

One way to account for the millimeter and submillimeter continuum is that there is an additional population of grains that radiate like blackbodies. Jura et al. (1995) have noted that in the Red Rectangle, a grain may have a radius larger than 0.02 cm if the particle is to remain in a gravitationally bound orbit. If the grain radius is a and if λ is the characteristic wavelength at which the light is emitted, the particles emit like blackbodies when $(2\pi a/\lambda) \geq 1$. Grains with a radius ≥ 0.02 cm act like blackbodies for temperatures greater than ~ 10 K.

For blackbody particles in an optically thin region, the temperature, T_{gr}, at distance, D, from the central star is given by

$$T_{\mathrm{gr}} = \{L_*(1-\omega)/[16\pi\sigma_{\mathrm{SB}} D^2]\}^{1/4} , \quad (3)$$

where L_* is the luminosity of the central star, σ_{SB} is the Stefan-Boltzmann constant, and ω is the albedo of the grains. If there is shielding of the dust grains, the temperature will be lower than this value. For the Red Rectangle, we expect that in an optically thin region

$$T_{\mathrm{gr}} = 87\phi^{-0.50}(1-\omega)^{0.25} . \quad (4)$$

The albedo of the large grains is unknown, but may be as high as 0.9 (e.g., Rouleau & Martin 1991; Pollack et al. 1994). In this case, the typical temperature of a big grain in the disk at $\phi = 1''$ is 50 K. If most of the grains emit at $T_{\mathrm{gr}} = 50$ K, the predicted value of $F_\nu(100\ \mu\mathrm{m})/F_\nu(1300)$ is much lower than the observed value of 150. A mixture of small and large grains could reproduce the observed value of $F_\nu(100\ \mu\mathrm{m})/F_\nu(1300\ \mu\mathrm{m})$.

We estimate a lower bound to the mass of dust, M_{du}, from the millimeter continuum flux, F_ν, from the expression

$$M_{\mathrm{du}} \geq (F_\nu \lambda^2 D_*^2)/(2kT_{\mathrm{gr}}\chi_\nu) , \quad (5)$$

where D_* is the distance from Earth to the object and χ_ν is the opacity of the grains (cm^2 g^{-1}). The composition and emissivity of the grains are quite uncertain. Jura (1986) has proposed for the grains in the outflows from carbon stars that $\chi_\nu(60\ \mu\mathrm{m}) = 150$ cm^2 g^{-1}. If we assume that this opacity varies as $\nu^{1.3}$ (Le Bertre, Gougeon, & Le Sidaner 1995), then we expect that $\chi_\nu(1300\ \mu\mathrm{m}) \approx 3$ cm^2 g^{-1}. If $T_{\mathrm{gr}} = 50$ K, then from equation (5), $M_{\mathrm{du}} \geq 10^{30}$ g. If the absorption opacity at 1.3 mm is lower than 3 cm^2 g^{-1} (see, for example, Pollack et al. 1994; Rouleau & Martin 1992), then the derived mass is larger.

The mass of dust required to explain the millimeter continuum appears to be significantly larger than the mass of dust required to account for the reflection nebulosity of the Red Rectangle, M_{scat}. Using models somewhat similar to those computed by Yusef-Zadeh, Morris, & White (1984), Lopez et al. (1995) successfully reproduce the image of the Red Rectangle and here, because they did not do so, we derive the mass of grains in their model. They employ a density distribution, $n(R, \theta)$ of the form

$$n(R, \theta) = n_0(R_{\mathrm{in}}/R)f(\theta) , \quad (6)$$

where R_{in} is the inner boundary of the dust, n_0 is a constant to be evaluated, and $f(\theta)$ is a function that describes the distribution of matter measured at polar angle θ away from the disk and $f(0) = 1$. Lopez et al. (1995) assume a single size for the grain size—a radius of 0.25 μm. Their model is characterized by the extinction optical depth, τ_{ext} measured through the plane of the disk which from equation (6) is given by

$$\tau_{\mathrm{ext}} = n_0 Q_{\mathrm{ext}} \pi a^2 R_{\mathrm{in}} \ln[R_{\mathrm{out}}/R_{\mathrm{in}}] , \quad (7)$$

where R_{out} is the outer boundary of the particle distribution. Lopez et al. (1995) suggest that at a wavelength of 1 μm, $\tau_{\mathrm{ext}} = 7$. They take $R_{\mathrm{in}} = 500$ times the stellar radius which implies, for $L = 1000\ L_\odot$ and $T_{\mathrm{eff}} = 8000$ K (Waelkens et al. 1992), that $R_{\mathrm{in}} = 6 \times 10^{14}$ cm (40 AU). (We note that this estimated inner radiius for the dust is close to the value estimated for the distance between the star and the CH^+.) The model nebula extends to a distance of 20″ or 10^{17} cm (~ 7000 AU) from the star; therefore, $R_{\mathrm{out}}/R_{\mathrm{in}} = 170$. With $Q_{\mathrm{ext}} = 2$, we derive from equation (7) that $n_0 = 5.8 \times 10^{-7}$ cm^{-3}. The expression for M_{scat} within a telescope beam of angular radius 9″ or a projected distance R_{beam} of

4.4×10^{16} cm (3000 AU) can be derived from equation (6) as

$$M_{\rm scat} = 2\pi R_{\rm beam}^2 R_{\rm in} n_0 m_{\rm gr} f_{\rm vol} , \quad (8)$$

where $m_{\rm gr}$ is the mass of each grain (or 1.3×10^{-13} g if the density of this material is 2 g $\rm cm^{-3}$; Rouleau & Martin 1991). In equation (8), the factor $f_{\rm vol}$ corrects for the flattened distribution of the matter for θ ranging between 0 and $\pi/2$. With $f(\theta)$ given by Lopez et al. (1995), $f_{\rm vol} \approx 0.50$. Using these parameters in equation (8), we find that $M_{\rm scat} = 3 \times 10^{29}$ g, about a factor of 4 lower than the minimum mass of dust required to produce the millimeter continuum.

From the models of Van der Veen et al. (1994) or Lopez et al. (1995) or from our Figure 6, we imagine that except for the radio emission, most of the energy emitted at wavelengths longward of 100 μm is produced by a population of cold grains that is distinct from the warmer grains that emit the infrared radiation at $\lambda < 100$ μm. At 100 μm, $\nu F_\nu = 2 \times 10^{-9}$ ergs $\rm cm^{-2}$ $\rm s^{-1}$ which is about 1% of the bolometric flux from the Red Rectangle. Because the warm grains absorb 97% of the energy emitted by the star (Sitko 1981), it seems that the warm grains absorb about 100 times as much energy as do the cold grains, even though there is about 10 times as much mass in the cold grains as there is in the warm grains. Either the distinct population of cold grains is confined to a very small volume, or these particles have a very low cross section per gram of material.

We tentatively suggest that the cold grains are large particles that are confined to a long-lived disk around the star. There are four reasons why we think that the millimeter and submillimeter continuum is produced by a distinct population of cold, large grains. (1) The morphology of the reflection nebulosity points toward the existence of a disk (e.g., Cohen et al. 1975). (2) The existence of such a long-lived disk is the easiest way to explain the abundances in the atmosphere of HD 44179. (3) In the wavelength range between 450 μm and 2 cm, F_ν varies as ν^{+2}. (4) Jura et al. (1995) report that the circumstellar CO profile in the Red Rectangle displays a narrow spike with a FWHM of 2 km $\rm s^{-1}$. If we assume that this gas lies in a circumstellar disk, then its orbital speed is ~ 1 km $\rm s^{-1}$. By the arguments used above to estimate the size of the region that produces the narrow spike in the Hα profile, we suggest that the region that produces the CO emission has a radius of 2×10^{16} cm (~ 1000 AU). It is plausible but uncertain that this slow-moving gas is associated with the cold dust responsible for the millimeter and submillimeter continuum.

If the same dust emits both the centimeter wavelength and millimeter wavelength continuum, then between 0.13 cm ($F_\nu = 250$ mJy) and 1.3 cm where the flux from dust is ≈ 3 mJy, the spectral index varies approximately as ν^{+2}. Although we do not know the temperature distribution of these grains, this spectral index suggests that the emissivity of the particles does not vary much between these two wavelengths, consistent with the hypothesis that at $\lambda = 0.13$ cm, $2\pi a/\lambda \geq 1$ and therefore that $a \geq 0.02$ cm.

4.2. *Possible Model*

Figure 7 displays a schematic picture for our model of the Red Rectangle. The central binary, HD 44179, contains some fast-moving ionized gas that produces the plateau in the Hα emission. However, most of the circumstellar matter is found at distances much larger than the binary separation. We imagine that there is a long-lived orbiting disk that largely consists of "big grains." In the inner portion of this disk, there is a blister of ionized gas and a photodissociation front with $\rm CH^+$. Around the disk, there is an extended halo of dust grains and neutral gas.

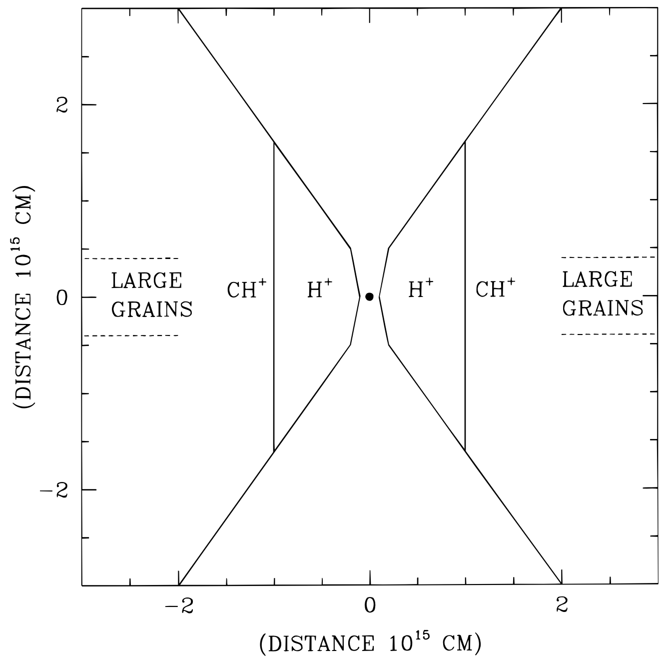

FIG. 7.—A schematic, edge-on, cutaway picture of the dust and gas around the Red Rectangle. The binary system, HD 44179, lies at the central dot. We presume that the high-velocity Hα (the plateau) lies in this close binary system while the Hα spike and radio continuum are produced in the zone denoted as $\rm H^+$ with the $\rm CH^+$ lying beyond the ionized hydrogen. We picture that the large grains are concentrated in a thin disk while the smaller grains are distributed in a much thicker, extended zone. The location of the observed CO is uncertain; it is not known whether it is concentrated in the disk or in a bipolar outflow.

We propose that the long-lived disk of orbiting particles has a total mass larger than 10^{30} g, and it contains particles with a typical radius near $a = 0.02$ cm. We imagine that in the orbiting disk, there are grain-grain collisions which lead both to grain growth (Chokshi, Tielens, & Hollenbach 1993) and grain fragmentation (Borkowski & Dwek 1995) with the creation and ejection of small particles as might occur around RAFGL 2688 (Jura & Kroto 1990). Therefore, in addition to this disk of large particles, there is an extended halo of particles to produce the reflection nebulosity. Those particles which have radii less than 0.02 cm can be driven out of the system by radiation pressure and may be responsible for the reflection nebulosity and much of the infrared radiation at wavelengths shortward of 100 μm (Lopez et al. 1995). In this picture, the dust in the reflection nebulosity has been ejected from the disk and not directly from HD 44179—consistent with the observation that it is currently an A-type star. There is no need to require the presence of a hitherto undetected mass-losing red giant (Roddier et al. 1995).

We suggest that the temperature of the large particles in this disk be near 50 K. These large, cold particles produce the millimeter and some of the submillimeter continuum from the Red Rectangle, but they do not emit much energy at wavelengths shortward of 100 μm. We display in Figure 6 the spectrum of a 50 K blackbody normalized so that F_ν(1.3 cm) = 3 mJy. Except at 450 μm, the agreement between this very simple model and the data is reasonable.

As discussed above, the outer radius of the disk of large grains is quite uncertain and may range from 3×10^{15} cm (200 AU) to 2×10^{16} cm (1300 AU). If the outer radius is 5×10^{15} cm (~ 300 AU), if the mass of cold particles is 10^{30} g and if the density is uniform, then the surface density of the disk is 0.01 g cm^{-2}. Therefore, if the grain emissivity at 1300 μm is 3 cm^2 g^{-1}, the vertical optical depth through the disk is 0.03; for comparison, the vertical optical depth derived from the geometric cross section of the grains is ~ 0.2. In either case, as expected, the disk is optically thin vertically. These proposed parameters for the spatial distribution of the big grains are very uncertain; more sophisticated models will be appropriate once we have more information about the spatial distribution of the millimeter and submillimeter flux. Finally, we speculate that there may exist in orbit around HD 44179 solid objects much larger than 0.02 cm in radius.

5. CONCLUSIONS

We report radio and optical measurements of the Red Rectangle with the following results.

1. The VLA emission is resolved in a compact and an extended source. The compact source is produced by circumstellar ionized gas with $n_e^2 V \geq 3 \times 10^{55}$ cm^{-3}. This ionized gas is largely confined to a region with a diameter between 1.3×10^{14} cm (~ 10 AU) and 2×10^{15} cm (~ 100 AU). We find that 10^6 cm$^{-3} \leq n_e \leq 4 \times 10^6$ cm^{-3}.

2. The ionized gas and the circumstellar CH^+ both appear to lie at about the same distance from the central star. A photodissociation front that started at least 40 yr ago may be propagating through the gas, consistent with a possible factor of 2 increase in the amount of ionized gas in the extended circumbinary region. The star may be in a rapid post-AGB evolutionary phase.

3. The extended radio emission has a spectral index between 3.6 cm and 1.3 cm ≥ 3.2; this emission is almost certainly produced by grains. It is possible, but not established, that the grains which emit the centimeter continuum also emit the previously detected millimeter continuum.

4. To account for the millimeter and much of the submillimeter continuum and the extended centimeter emission, we tentatively propose that there is a long-lived gravitational bound disk around HD 44179 whose outer radius is between 3×10^{15} cm (200 AU) and 2×10^{16} cm (~ 1300 AU) and which consists of orbiting particles with radii ≥ 0.02 cm whose typical temperature is near 50 K.

We thank Schuyler Van Dyck for helpful discussions and assistance with AIPS, and Cecilia Barnbaum for assistance in using IRAF to reduce the Lick data. We thank Gary Schmidt for reexamining his old data and Mark Claussen for informing us about his VLA measurements with A. Beasley before publication. M. J.'s work has been partly supported by NASA while J. T.'s work has been partly supported by the NSF.

REFERENCES

Alcolea, J., & Bujarrabal, V. 1991, A&A, 245, 499
———. 1995, A&A, 303, L21
Balm, S. P., & Jura, M. 1992, A&A, 261, L25
Blondel, P. F. C., Talavera, A., & Djie, H. R. E. T. A. 1993, A&A, 268, 624
Borkowski, K. J., & Dwek, E. 1995, ApJ, 454, 254
Bregman, J. D., Rank, D., Temi, P., Hudgins, D., & Kay, L. 1993, ApJ, 411, 794
Chokshi, A., Tielens, A. G. G. M., & Hollenbach, D. 1993, ApJ, 407, 806
Claussen, M. J., & Beasley, A. 1995, private communication
Cohen, M., et al. 1975, ApJ, 196, 179
Gottlieb, E. W., & Liller, W. 1976, ApJ, 207, L135
Greenstein, J. C., & Oke, J. B. 1977, PASP, 89, 131
Griffin, I. P. 1990, MNRAS, 247, 591
Hillenbrand, L. A., Strom, S. E., Vrba, F. J., & Keene, J. 1992, ApJ, 397, 613
Hummer, D. G., & Storey, P. J. 1987, MNRAS, 224, 801
Ivezic, Z., & Elitzur, M. 1996, MNRAS, 279, 1019
Johnson, H. L. 1966, ARA&A, 4, 193
Jura, M. 1986, ApJ, 303, 327
———. 1994, ApJ, 434, 713
Jura, M., Balm, S., & Kahane, C. 1995, ApJ, 453, 721
Jura, M., & Kroto, H. 1990, ApJ, 351, 222
Kelly, D. M., & Latter, W. B. 1995, AJ, 109, 1320
Knapp, G. R., Bowers, P. F., Young, K., & Phillips, T. G. 1994, ApJ, 429, L33
———. 1995, ApJ, 455, 293
Koerner, D. W., Chandler, C. J., & Sargent, A. I. 1995, ApJ, 452, L69
Le Bertre, T., Gougeon, S., & Le Sidaner, P. 1995, A&A, 299, 791
Léger, A., & Puget, J. L. 1984, A&A, 137, L5
Lissauer, J. L., Wolk, S. J., Griffith, C. A., & Backman, D. E. 1996, ApJ, 465, 371
Lopez, B., Mékarnia, D., & Lefèvre, J. 1995, A&A, 296, 752
Mannings, V., & Emerson, J. P. 1994, MNRAS, 267, 361
Martin, P. G., & Rogers, C. 1987, ApJ, 322, 374
Mathis, J. S., & Lamers, H. J. G. L. M. 1992, A&A, 259, L39
Pollack, J. B., Hollenbach, D., Beckwith, S., Simonelli, D. P., Roush, T., & Fong, W. 1994, ApJ, 421, 615
Price, S. D., 1988, PASP, 100, 171
Reid, M. J., & Menten, K. M. 1995, in Radio Emission from the Stars and the Sun, ed. A. R. Taylor & J. M. Parades (ASP Conf. Ser.), in press
Roddier, F., Roddier, C., Graves, J. E., & Northcott, M. J. 1995, ApJ, 443, 249
Rouleau, F., & Martin, P. G. 1991, ApJ, 377, 526
Schmidt, G. D. 1995, private communication
Schmidt, G. D., Cohen, M., & Margon, B. 1980, ApJ, 239, L133
Schmidt, G. D., & Witt, A. N. 1991, ApJ, 383, 698
Shenton, M., Evans, A., & Williams, P. M. 1995, MNRAS, 273, 906
Sitko, M. L. 1981, ApJ, 247, 1024
———. 1983, ApJ, 265, 848
Sitko, M. L., Savage, B. D., & Meade, M. R. 1981, ApJ, 246, 161
Skinner, C. J. 1994, MNRAS, 271, 300
Skinner, S. L., Brown, A., & Stewart, R. T. 1993, ApJS, 87, 217
Spitzer, L. 1978, Physical Processes in the Interstellar Medium (New York: Wiley)
Taylor, A. R., Waters, L. B. F. M., Bjorkman, K. S., & Dougherty, S. M. 1990, A&A, 231, 453
Tielens, A. G. G. M., & Hollenbach, D. 1985, ApJ, 291, 722
van der Veen, W. E. C. J., Omont, A., Habing, H. J., & Matthews, H. E. 1995, A&A, 295, 445
van der Veen, W. E. C. J., Waters, L. B. F. M., Trams, N. R., & Matthews, H. E. 1994, A&A, 285, 551
Van Winckel, H. 1995, Ph.D. thesis, Katholieke Universiteit Leuven
Van Winckel, H., Mathis, J. S., & Waelkens, C. 1992, Nature, 356, 500
Van Winckel, H., Waelkens, C., & Waters, L. B. F. M. 1995, A&A, 293, L25
Waelkens, C., Van Winckel, H., Trams, N. R., & Waters, L. B. F. M. 1992, A&A, 256, L15
Walmsley, C. M., Chini, R., Kreysa, E., Steppe, H., Forveille, T., & Omont, A. 1991, A&A, 248, 555
Waters, L. B. F. M., Trams, N. R., & Waelkens, C. 1992, A&A, 262, L37
Waters, L. B. F. M., Waelkens, C., Mayor, M., & Trams, N. R. 1993, A&A, 269, 242
Yusef-Zadeh, F., Morris, M., & White, R. L. 1984, ApJ, 278, 186